Reflectional symmetry breaking of the separated flow over three-dimensional bluff bodies

Mathieu Grandemange and Olivier Cadot

ENSTA-UME, Unité de Recherche en Mécanique, Chemin de la Hunière, 91761 Palaiseau Cedex, France

Marc Gohlke

Department of Research and Innovation, PSA Peugeot-Citroën, 2 route de Gisy, 78943 Vélizy-Villacoublay, France

Experimental observation of a permanent reflectional symmetry breaking (RSB) is reported for a laminar three-dimensional wake. Based on flow visualizations, a first bifurcation from the trivial steady symmetric state to a steady RSB state is characterized at Re = 340. The RSB state becomes unsteady after a second bifurcation at Re = 410. It is found that this RSB regime is persistent at large Reynolds numbers and is responsible for a bistable turbulent wake.

Many industrial flows are produced by the motion of bluff bodies with a geometry of reflectional symmetry. The simplest cases that are frequently used can be found in the transport industries, especially for ground vehicles such as trains, cars, or lorries. The bluffness associated with the functional blunt shape provokes a massive flow separation and consequently a complex wake dynamics. Recently, bistability properties of such three-dimensional turbulent wakes have been reported in very distinctive geometries [1,2]: Each equiprobable state breaks the reflectional symmetry of the body but leads together to a statistically symmetric flow. This phenomenon reminds of symmetry breaking found in closed cell geometry [3] and may be a general property of turbulent flows. On the other hand, reflectional symmetry breaking (RSB) has been recently reported numerically in the bifurcation scenario of a disk wake at low Reynolds numbers [4,5]. A first bifurcation to a stationary mode also observed experimentally [6–8] selects a planar symmetry. Then the RSB appears as a Hopf bifurcation at Re = 123.7 from the development of two counter-rotating spiral modes, in addition to the previous stationary mode leading to a periodic shedding. The reflectional symmetry is finally restored for Reynolds number over 143.7 with the restabilization of the stationary mode. However, experimental evidence of this RSB is lacking, probably because of the small magnitude of asymmetry [4,5].

To our knowledge, experiments about bifurcations and symmetry breaking of the flow around three-dimensional (3D) bluff bodies with reflectional symmetry are needed. The present Rapid Communication investigates the flow around a basic body that is generally used to mimic car aerodynamics at Reynolds numbers ranging from 10^4 in laboratory experiments to 10^7 in real scale. It is shown, by means of flow visualizations, that this simple geometry provokes at low Reynolds numbers a bifurcation in the flow solution to a state that breaks the reflectional symmetry. The corresponding regime is persistent at large Reynolds numbers and responsible for the bistable property of the turbulent wake.

The three-dimensional body is described in Fig. 1. The Reynolds number $Re = \frac{UH}{\nu}$ is based on the height $H = 26$ mm of the body, the main flow velocity U_0, and the kinematic viscosity ν of the working fluid. The width $W = 1.35H$ and the length $L = 3.625H$ are set to reproduce a standard car [9].

First, the body is placed in a low speed hydrodynamics tunnel at a ground clearance $C = 0.6H$. Two dye injectors located behind the two backward supports are used to visualize the recirculating flow that forms at the trailing edge (see Fig. 1). The Reynolds number varies between 260 and 1300, adjusting abruptly the main flow velocity in the range 1 cm s^{-1} < U_0 < 5 cm s^{-1}; the precision due to the accuracy of reading the rotameter is $\Delta Re = \pm 10$. The dye is continuously injected with a syringe in such a way that the dye velocity at the exit of the injector never exceeds 10% of the main velocity. The tunnel has transparent walls, and it is also designed to visualize the wake in the flow direction (see Ref. [10] for a full description of the tunnel). Pictures are taken once the dye has filled the recirculating bubble. In the following, z_W, which denotes the mean position of the wake in the z direction, is used as a parameter of order. It is measured as the mean position of the dye trail downstream from the recirculation bubble by image analysis of the top view picture, and its precision is $0.02W$.

At the lowest Reynolds numbers, a steady symmetric regime (SS) is observed as depicted in Fig. 2(a) for Re = 310. The flow preserves the planar symmetry of the geometry and the presence of the ground induces a top-bottom asymmetry of the wake. This state remains stable up to Re = 340.

Past this critical Reynolds number, the wake starts to oscillate periodically in the plane of symmetry, as shown in Fig. 2(b). The structure of this unsteady symmetric regime (US) perfectly preserves the reflectional symmetry of the body, as can be stated by the corresponding top and rear views. It is associated with alternative loops that are shed from the top and bottom shear layers. However, this US regime is not permanent. Indeed, keeping the Reynolds number constant, this periodic shedding is progressively moving off the reflectional plane of symmetry: z_W varies slowly around 0 with a characteristic time evolution of 1 min, i.e., roughly ten shedding periods. Then the wake selects randomly one orientation and stabilizes to an asymmetric position, typically after a duration of 10 min. There, the oscillations get attenuated and the flow reaches a steady asymmetric regime (SA) denoted as $+$ or $-$ depending on the sign of z_W, which indicates the wake shift in the z direction. Figure 2(c) describes this steady state SA$^+$ that breaks the reflectional symmetry for Re = 365. Naturally, both SA$^+$ and SA$^-$ can be observed by repeating
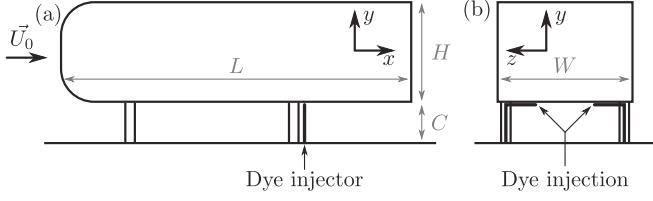
FIG. 1. Geometry of the model: (a) Side view and (b) rear view. For the low Reynolds number experiment, fluorescent dye is injected through two pipes behind the backward supports.

the Reynolds number increase from the SS regime without any intervention on the setup. This regime was stable over 2 h of observation; it is considered steady in the limit of the visualization means and water tunnel stability.

Eventually, when increasing the Reynolds number over 410, the SA wake starts to oscillate again as visible in Fig. 2(d) and leads to an unsteady asymmetric regime (UA). The flow preserves its orientation so that SA$^+$ turns into UA$^+$ and similarly SA$^-$ becomes UA$^-$. Hence, Figs. 2(c) and 2(d) were obtained for two different experiments of the Reynolds number increase. The top view in Fig. 2(d) shows that the oscillations are concentrated only on one side of the body but its dynamics is complex. The unsteadiness is associated with oscillations in both the y and the z directions. It is then probable that two different frequencies coexist, as observed in the turbulent wake
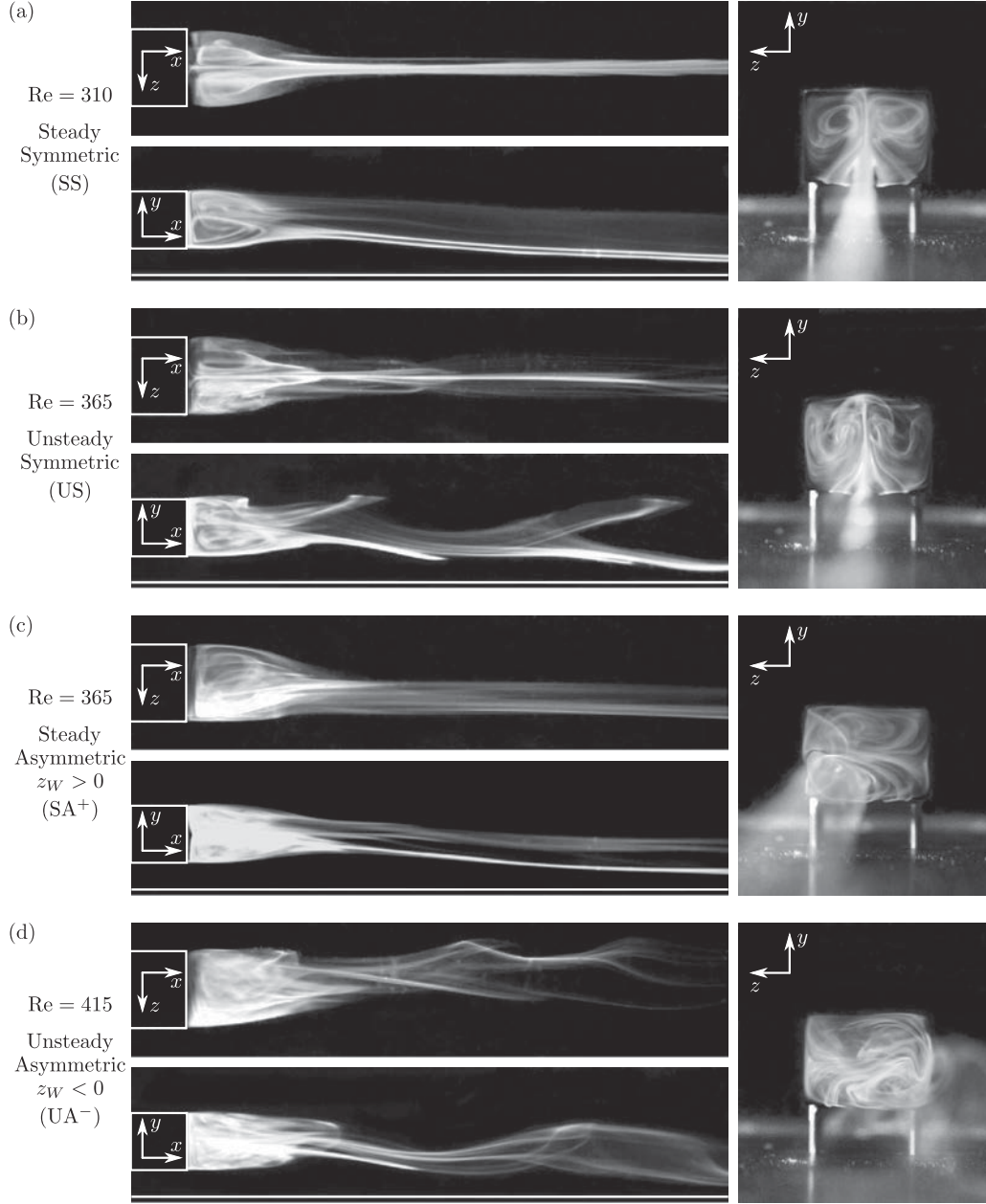

FIG. 2. Flow visualizations at the Reynolds numbers (a) Re = 310, (b) and (c) Re = 365, and (d) Re = 415. For each Reynolds number: Top picture, top view; bottom picture, side view; right picture, rear view. The flow comes from the left for both top and side views. Regimes observed in (a), (c), and (d) are permanent states while (b) is a transient state. Observations in (c) and (d) have been obtained from different experiments of Re increase in order to show both states for which $z_W < 0$ and $z_W > 0$.
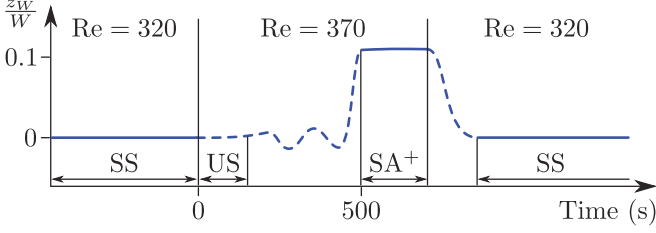
FIG. 3. (Color online) Typical evolutions of the wake positions z_W during a Reynolds number increase from 320 to 370 followed by a decrease back to 320: Continuous lines, permanent states; dashed lines, transient states.

of elliptical and rectangular flat plates [11]; one is associated with the interaction of the top-bottom shear layers and the other with the interaction of the lateral ones. However, the setup does not allow a reasonably precise measurement of the oscillation amplitudes and frequencies in the cross-flow plane. Eventually, the spontaneous migration between the regimes UA^+ and UA^- was not observed but can be induced by energetic perturbations such as short time suppression of the free flow.

After a decrease of the Reynolds number, the flow goes from UA to SA at Re = 410 and then directly to the SS state as soon as the Reynolds number gets smaller than 340, so that the US regime is never observed. This behavior is summarized through the typical evolution of the wake shift z_W in Fig. 3.

It is worth mentioning that during the transition from SS to SA, the US regime is always reported. This tends to indicate that imperfections of the shedding of the US regime are needed to initiate slight asymmetries, and this transient regime then loses slowly its intensity while the wake continuously moves off axis to eventually reach the SA regime.

From these observations, the bifurcation scenario presented in Fig. 4 is proposed to classify the different stable regimes: SS for Re < 340, SA for 340 < Re < 410, and UA for Re > 410. The US regime is displayed as an unstable state as it is transient and only visible between SS and SA. The evolution of the parameter of order with Re confirms the presence of a pitchfork bifurcation at Re = 340.

The same geometry is now placed in a wind tunnel at a free-stream velocity of $U_0^T = 20$ m s^{-1}. The flow is now turbulent and the associated Reynolds number is 9.5×10^4. The ground clearance is set at $0.2H$ to approach the reference experiments of Ahmed *et al.* [9]. Besides, as the effect of the viscous forces is strongly attenuated compared to
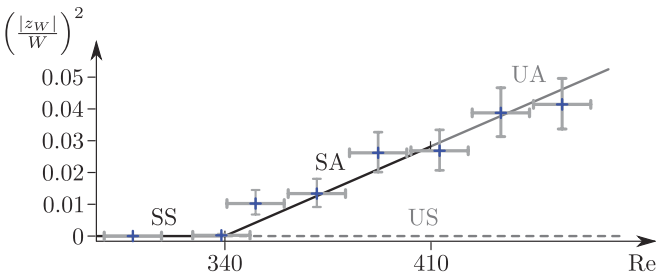

FIG. 4. (Color online) Bifurcation scenario of the wake: Black and gray lines are steady and unsteady regimes, respectively, continuous and dashed lines are stable and unstable regimes, respectively, and crosses are experimental measurements and error bars.
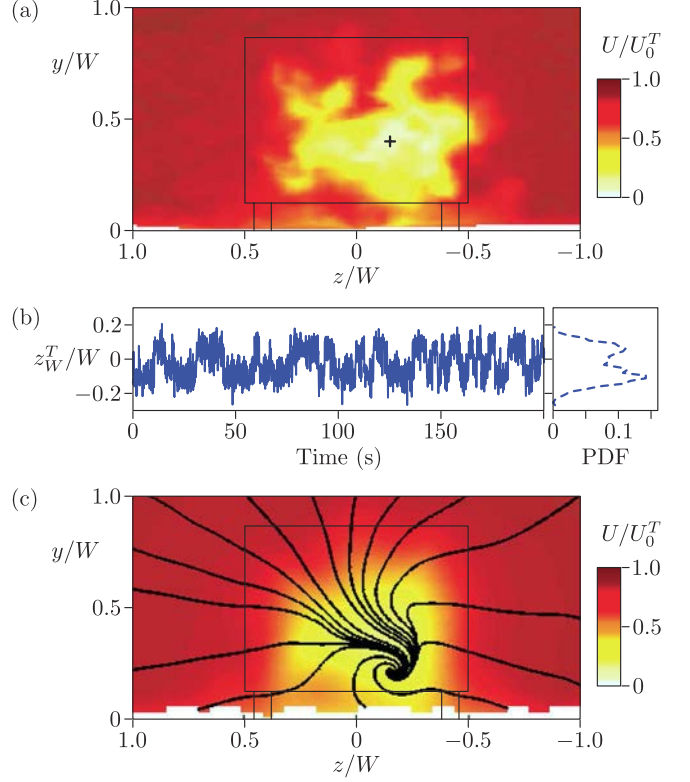

FIG. 5. (Color online) (a) Instantaneous streamwise velocity in the turbulent wake at $x = 1.5W$, and the cross locates the barycenter of momentum deficiency at $y_W^T = 0.40W$ and $z_W^T = -0.15W$. (b) Time evolution of the turbulent wake position z_W^T from 2000 snapshots recorded at 10 Hz (left) and its associated probability density function (right). (c) Mean streamlines are colored by streamwise velocity at $x = 1.5W$; velocities are averaged from the snapshots where $z_W^T < 0$.

the precedent experiments, the intensities of the underbody flow are comparable despite the ground clearance difference. Stereo-particle image velocimetry (PIV) is performed in the wake at $x = 1.5W$ and used to locate the barycenter of momentum deficiency in this cross-flow plane. A snapshot displayed in Fig. 5(a) presents the turbulent wake off the reflectional plane of symmetry, located at $y_W^T = 0.40W$ and $z_W^T = -0.15W$.

The analysis of the 2000 velocity fields recorded at 10 Hz leads to the time evolution of the z_W^T presented in Fig. 5(b). The probability density function clearly shows the presence of two preferred positions $z_W^T \approx \pm 0.1W$: The wake is either oriented to the positive or negative z direction. Conditional averaging on z_W^T enables the asymmetric topologies to be obtained; similar wake offsets in the z direction are observed in the $z_W^T < 0$ asymmetric state displayed in Fig. 5(c) and in the UA^- regime shown in Fig. 2(d). Topology shifts are observed after a typical duration of 5 s, which is long compared to the expected shear layer dynamics at a Strouhal number of around 0.2, corresponding roughly to 50 Hz in these experiments. These shifts seem to occur randomly so that the mean flow statistically retrieves the symmetry of the setup.

As a conclusion, this Rapid Communication reports experimental evidence of the reflectional symmetry breaking (RSB)

in three-dimensional laminar wakes: The bifurcation scenario of the wake presents asymmetric permanent regimes. The SA and UA regimes have equal probability of being shifted toward the $z > 0$ or $z < 0$ regions. The transient US regime seems necessary to initiate slight asymmetries of the flow to reach the permanent SA or UA regimes. Further work improving the measurement technique could clarify the amplitude and frequencies of the oscillations in the y and z directions. It could also confirm whether both oscillations emerge simultaneously and whether the transition from SA to UA is a Hopf bifurcation.

Besides, it is found that the bifurcation scenario strongly depends on the ground clearance: The steady RSB regime is not reported for $C < 0.4H$. It may depend on the top-bottom recirculation balance: A particular three-dimensional arrangement of the different shear layers is certainly needed and remains to be clarified. The condition of the appearance of RSB regimes is of fundamental interest as it may induce a significant side force and then additional drag.

Signatures of these permanent symmetry breaking regimes are also found at larger Reynolds numbers. If spontaneous migrations between UA$^+$ and UA$^-$ are unlikely to happen in laminar regimes, the energetic large scale structures of turbulence should certainly induce natural migrations in a random way. While the RSB is clearly evidenced for wakes of ground vehicles by the present work and by the experiments of Lawson *et al.* [1], we believe it to be much more general and observed in other types of wake flows. For instance, some asymmetry in the hull wake behind a container ship has been reported [12] despite huge efforts by the authors to respect the reflectional symmetry.

Eventually, these results point out the limits of the common procedure consisting in implementing the instrumentation of a blunt geometry based on its reflectional symmetries. In terms of three-dimensional unsteady simulations, reduced physical times of the calculation may also prevent the flow from reaching permanent asymmetric regimes.

[1] N. J. Lawson, K. P. Garry, and N. Faucompret, Proc. Inst. Mech. Eng., Part D **221**, 739 (2007).

[2] B. Herry, L. Keirsbulck, L. Labraga, and J. Paquet, J. Fluids Eng. **133**, 054501 (2011).

[3] F. Ravelet, L. Marie, A. Chiffaudel, and F. Daviaud, Phys. Rev. Lett. **93**, 164501 (2004).

[4] D. Fabre, F. Auguste, and J. Magnaudet, Phys. Fluids **20**, 051702 (2008).

[5] P. Meliga, J. Chomaz, and D. Sipp, J. Fluid Mech. **633**, 159 (2009).

[6] H. Sakamoto and H. Haniu, J. Fluids Eng. **112**, 386 (1990).

[7] D. Ormières and M. Provansal, Phys. Rev. Lett. **83**, 80 (1999).

[8] P. Szaltys, M. Chrust, A. Przdka, S. Goujon-Durand, L. S. Tuckerman, and J. E. Wesfreid, J. Fluids Struct. **28**, 483 (2012).

[9] S. Ahmed, G. Ramm, and G. Faitin, SAE Technical Paper No. 840300, doi:10.4271/840300 (1984).

[10] B. Thiria, S. Goujon-Durand, and J. E. Wesfreid, J. Fluid Mech. **560**, 123 (2006).

[11] M. Kiya and Y. Abe, J. Fluids Struct. **13**, 1041 (1999).

[12] J. Y. Lee, B. G. Paik, and S. J. Lee, Ocean Eng. **36**, 377 (2009).